PROCEEDINGS OF SPIE

SPIEDigitalLibrary.org/conference-proceedings-of-spie

Cold shaping of thin glass foils: a fast and cost-effective solution for making light-weight astronomical x-ray optics

Civitani, M., Basso, S., Citterio, O., Ghigo, M., Salmaso, B., et al.

M. M. Civitani, S. Basso, O. Citterio, M. Ghigo, B. Salmaso, G. Pareschi, G. Vecchi, "Cold shaping of thin glass foils: a fast and cost-effective solution for making light-weight astronomical x-ray optics," Proc. SPIE 9603, Optics for EUV, X-Ray, and Gamma-Ray Astronomy VII, 960310 (21 September 2015); doi: 10.1117/12.2188580

Event: SPIE Optical Engineering + Applications, 2015, San Diego, California, United States

Cold shaping of thin glass foils: a fast and cost-effective solution for making light-weight astronomical x-ray optics

M. M. Civitani[a,1], S. Basso[a], O.Citterio[a], M. Ghigo[a], B. Salmaso[a], G. Pareschi[a], G.Vecchi[a]

[a]INAF Astronomical Observatory of Brera, Via E. Bianchi 46, I-23807 Merate (LC), Italy

ABSTRACT

Recent advancements in thin glass materials allowed the development and the mass production of very thin glass foils, like e.g. the Willow glass (thickness of 0.1-0.2 mm) produced by Corning or AF32 produced by Schott (thickness down to 0.055 mm). The thickness, strength and flexibility of these glass foils allow bending them up to very small radius of curvature without breaks. This feature, together with the very low micro-roughness, makes this kind of materials ideal candidates for pursuing a cold replication approach for cost-effective and fast making of grazing incidence astronomical optics. Starting from the very thin flat glass sheets, the process under development foresees to bond them onto the supporting structure while they are wrapped around reference mandrels. The assembly concept, based on the use of Wolter-I counter-form moulds, is also based on the use of reinforcing ribs that connect pairs of consecutive foils in the final assembly. The ribs do not only play the role of mechanical connectors, they keep the shape and increase the structural stiffness. Indeed, the ribs constrain the foil profile to the correct shape during the bonding, damping the low-frequency residuals with respect to the Wolter I configuration. This approach is particularly interesting because of their low weight and cost. They could e.g be used for the production of high throughput optics as those needed for the Chines XTP mission, in which the requirements on the angular resolution are not too tight. In fact, a Half Energy Width in the range of 20-60 arcsec is compatible with the expected residual error due to the spring back of the glass sheets. In this paper we provide an overview of the project, the expected performances and present the first preliminary results.

Keywords: X-ray segmented optics, cold slumping replication, integration and alignment of glass foils optics

1 INTRODUCTION

Since several years, the slumped glass optics (SGO) has been developed for the realization of x-ray optics. With the realization of NuSTAR telescope [1], it can be considered well-proven and mature technology. It mainly relies on two process steps. The glass segments are produced with hot slumping technique and they are assembled into modules through integration. The different groups in Europe and in US have developed different hot slumping techniques [2,3]. As well, different integration concepts are under study [4,5].

The new mirror realization concept, illustrated in this paper, follows partially the approach developed at INAF/OAB [6] and related to the realization of XOU for large mirror assemblies, like ATHENA [7]. In this case, however, the first part of the process, the hot slumping of the glass, is skipped. Usually, in the SGO related activities, the segmented glass of 0.4 mm thickness are shaped via hot slumping in cylindrical configuration before being figured in Wolter-I configuration with the cold slumping approach during the integration. In this case hot slumping (at a temperature between 550°C and 750°C depending on the type of glass) is necessary for the stress release, as the desired angular resolution is of few arcsec. On the opposite, in all the cases in which the requirements in terms of angular resolution are not so tight, the hot slumping process can be avoided. In these cases, the initial shape of the glass will be farer from the theoretical one and the residual spring back of the glass greater. Nevertheless, as the tolerances on the profile error are loose, it is possible to tune the process, almost in terms of glass thickness and constrain scheme, so that the final shape of the glass is compatible with the requirements. This 'cold slumping glass optics' concept has been patented (TO2015A000219).

The process under development starts from the thin flat glass sheets: they are bonded onto the supporting structure while they are wrapped around reference mandrels. This assembly concept is based on the use of double-conical or Wolter-I

[1] Corresponding author: marta.civitani@brera.inaf.it; phone +39-039-5971028; fax +39-039-5971000; www.brera.inaf.it

Optics for EUV, X-Ray, and Gamma-Ray Astronomy VII, edited by Stephen L. O'Dell, Giovanni Pareschi,
Proc. of SPIE Vol. 9603, 960310 · © 2015 SPIE · CCC code: 0277-786X/15/$18 · doi: 10.1117/12.2188580

counter-form moulds and on the use of reinforcing ribs. These ribs connect pairs of consecutive foils in the final assembly, playing the role of mechanical connectors: they keep the shape of the foil and increase the structural stiffness. Indeed, the ribs constrain the foil profile to the correct shape during the bonding, damping the low-frequency residuals with respect to the counter-form configuration.
The recent advancements in thin glass materials allow the development and the mass production of very thin glass foils. As example Corning produces Willow glass with thickness of 0.1-0.2 mm, while Schott realizes the AF32 with thickness down to 0.055 mm. The thickness, strength and flexibility of these glass foils allow bending them up to very small radius of curvature without breaks. This feature, together with the very low micro-roughness, makes this kind of materials ideal candidates for pursuing a cold replication approach for cost-effective and fast making of grazing incidence astronomical optics.
Differently from the NuSTAR glass mirrors [1], which have been slumped before the integration, in this case the choice of a suitable glass thickness and the particular integration procedure allow to keep the stress in the glass under security limit.
Moreover, starting from flat glasses and avoiding the hot slumping process, the initial micro-roughness of the glass is preserved. This is more important for high energy application, at energies greater than 10keV: in these cases the cold replication approach represent a key process and is very attractive for many high-throughput optics applications.
The advantages of this new approach are the low weight and the low cost of the optics. As the hot slumping procedure is skipped, the realization costs are highly reduced, both for the slumping mandrel procurement cost, and for the overall production time. This concept could be used for the production of high throughput optics in which the requirements on the angular resolution are not too tight: a Half Energy Width in the range of 20-60 arcsec is fully compatible with the expected residual error due to the spring back of the glass sheets.
In this paper we provide an overview of the project, the expected performances and presents the first preliminary results.

2 INTEGRATION CONCEPT

As anticipated in the previous paragraph, the integration concept is the same followed for the SGO. Hereafter it is briefly summarized. The integration concept is based on the fundamental assumption that under a vacuum suction the plate can assume the shape of the forming mould. If the mould profile was previously precisely figured to the negative shape of the reflecting surface to be achieved, the glass plate, fixed in this configuration, has the ideal shape: gluing the ribs as spacers between consecutive glass plates, it can be assembled in a stack. These ribs will guarantee the strength of the XOU and will keep the plates in the right position and shape. The differences between the shape of the glass plate and forming mould introduce deformations in the glass plate as spring back effect after the glass plate release. The amplitude and the shape of these deformations are mainly function of the initial shape of the glass, of the radius of curvature and of the thickness of the glass [8].

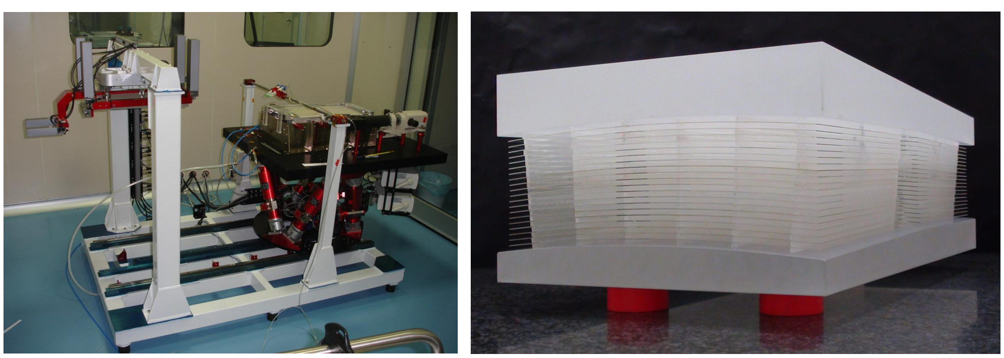

Figure 1: The Integration Machine (IMA) in INAF/OAB laboratories and the X-ray Optical Unit Breadboard (XOU_BB) [11]

From a general point of view, in order to avoid local deformations in the glass, particular care has to be taken in the cleaning in order not to trap dust grains between the mould and the glass [9]. In a perfect cold shaping process, the optical surface of the glass is kept in contact with the mould and the mould itself may be taken as a reference during the alignment of the plates in the stack. For this reason this integration scheme is called "mould integration". Using the mould measurement, each plate pairs will be firstly aligned and then integrated into the stack by gluing it to the previous plate pair. The machining of the ribs does not precisely follow the curved rear of the figured glass plate surface: they are just tapered to a coarse conical profile. The glue that will fill the gap between the glass and the ribs will compensate all the differences in profiles at macro and microscopic level. The glue thickness layer is around 50micron that corresponds to the optimal values for the toughness and adherence of the glues (this aspect has been proven after careful experimental tests). The position and the orientation of the moulds are carefully measured with a 3D machine: the measurement points acquired on the optical surface of the integration molds are used to align together the parabolic mould with respect to the hyperbolic mold. The relative alignement and position is recorded and can be re-stored by means of picomotors actuators that works in close loop with two autocollimators and a capacitive sensor. A simplification in the integration procedure could be the use of a monolithic mould of parabola and hyperbola. The same scheme can be adopted, but the relative orientation of the two plates will not be matter of integration but of mould realization.

At the moment, the stacking process is focused on the assembly of XOU, azimuthal and radial partition of a greater mirror assembly. The procedure is operated with the Integration Machine (IMA) [10], a semi-robotic system, developed in the context of an ESA contract from 2009 to 2013. It is commonly used with thin glass foils (0,4mm thick) previously shaped with hot slumping. It combines the cold replication approach and a very tight alignments capability. Very precise sensors (autocollimators and linear transducers) and differential measurement approach permit to achieve a sub-micron alignment between the hyperbolic and parabolic sectors of a Wolter-I optic and few arcsec between each pair plate. It is installed in the INAF/OAB labs in a clean room area with a temperature control of +/-0.2 degree. In figure 1 are shown the IMA and a prototypal optics realized with it [11].

The IMA is already fully compatible with the cold slumping proposed integration concept: as descripted in the paragraph 5, it has been already used to build a very simple demonstrator based on Willow flat glasses.

Instead, for creating complete azimuthal modules with low radius of curvature, some parts of the IMA need to be modified. The new conceptual design is shown in figure 2. In the left panel, the central part of the telescope, hereafter called mandrel, is in orange. The introduction of a rotational movement around a central mandrel allows the integration of foils all-around the central axis. The integration molds are in this case concave and the integration will be carried out placing the backside of the glass in contact with the molds. This 'indirect integration approach' does not introduce particular problem as soon as the thickness variation on the glass are compatible with the required result. It has been already proven with the JIM integration [9] without issues.

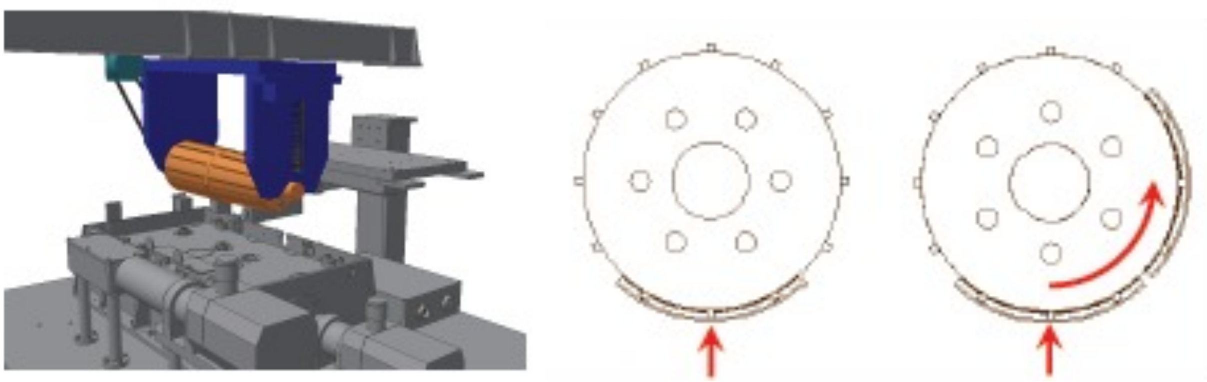

Figure 2: The changes in the IMA set-up to assemble mirror module with small radius of curvature: a rotary movement is introduced allowing the glass stacking around the central mandrel.

The stress of the glass in the final integrated configuration, depends on several factors as its size, its thickness, the geometry of the constrain and the difference between its intrinsic shape and the one of the integration mold. Each of these parameters can be optimized as a function of the results to be achieved by means of FEM simulations. Assuming 200mm x200mm^2 size, an integration mold with radius of curvature ranging between 100 and 1000mm, a focal length of 4.5m, the stresses for 0.2mm (red) and 0.1mm (blue) thickness glasses have been calculated. The results are shown in figure 3. In all these cases, six bonded ribs have been modeled as constrain points. Moreover, different intrinsic errors of the glass foils are considered, the initial peak-to-valley being 100microns and 10microns. The introduced stress grows exponentially for smaller radius of curvature while it is slightly correlated with the initial peak-to-valley. In order to maintain an acceptable level of stress in the bent glass, the lower is the radius of curvature, the lower is the needed glass thickness.

On the other side, the expected HEW of the integrated sample is almost linear with the initial peak-to-valley of longitudinal errors on the glass: it ranges between 20" and 40" in single reflection if the glass longitudinal error is around 10micron peak-to-valley. As soon as the configuration of the mirror module is fixed, optimization for glass size and ribs patterns can be carried out in order to achieve the desired optical performances.

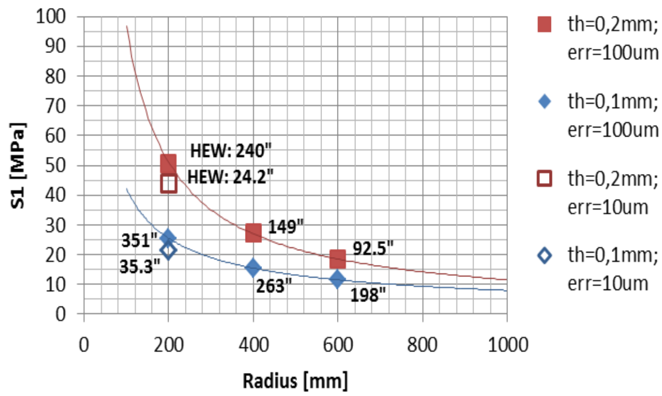

Figure 3: Maximum stress in a flat glass integrated with cold slumping approach after the vacuum release, and expected HEW of the integrated samples

3 SUBSTRATE CHARACTERIZATION

The characterization of the substrates started with the Willow glass produced by Corning. Few segments of glasses (hereafter called sample A, B, C and E, have been purchased already cut into a dimension suitable with our present integration set-up: they are 200mm x 200mm as the slumped glass produced in INAF/OAB. In order to acquire confidence with thin glasses handling, it has been decided to start with 200microns thickness, the half of the thickness up to now considered for the slumping. These segments have been analyzed in terms of initial figure error, thickness variation and micro-roughness. The obtained results are reported in the following.

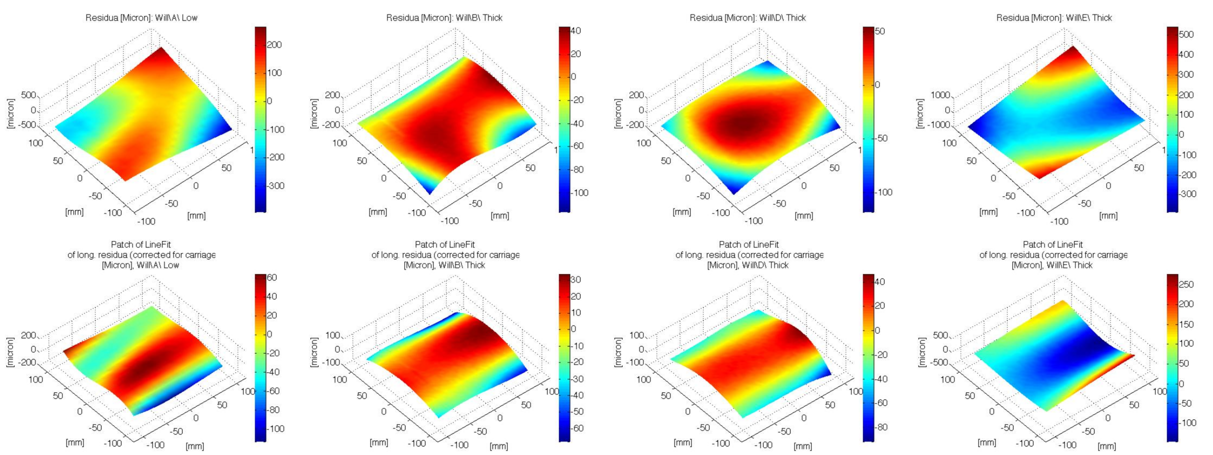

Figure 4: The residua with respect to a plane and along the vertical direction as measured on the four samples considered.

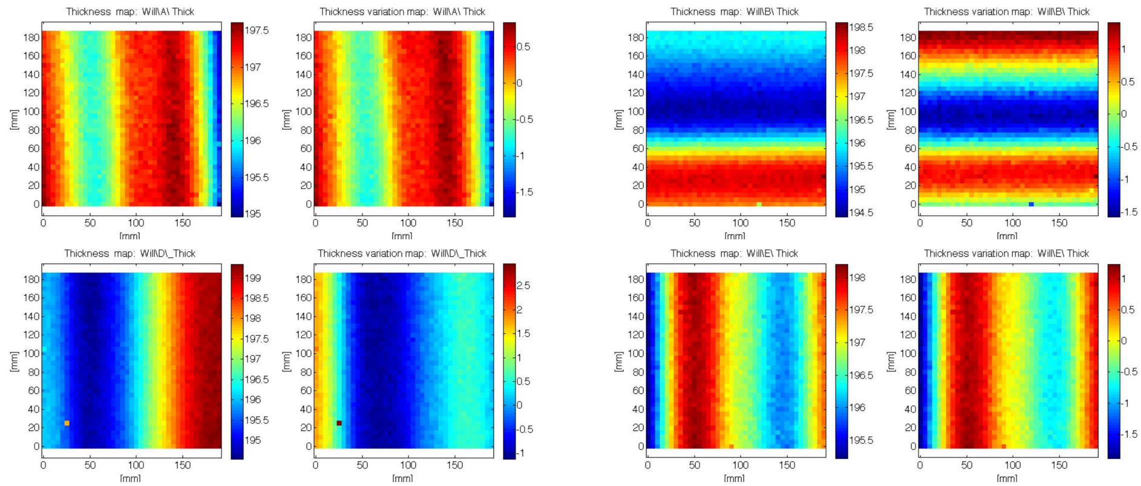

Figure 5: The thickness and the thickness variation as measured by the CUP on the four Willow samples. The color scale in the images is in microns.

Due to the small thickness, the glasses are very floppy and their intrinsic shape is difficult to be known with high accuracy. A 3D map of the surface has been acquired with the CUP [12], the glass foil being in vertical position. The glasses have been supported on the bottom on two points, while one constrain point is placed in the central top part of the glass. The amount of the gravity deformation expected in this configuration is of few microns peak-to-valley, but as the intrinsic errors measured are of an order of magnitude higher they are not subtracted at the moment. In figure 4 are reported the overall residua with respect to a plane on the different glasses and the longitudinal profile error in the vertical direction. The total peak-to-valley is of around 200microns in almost all the cases, while along the vertical direction the error is of the order of 100 microns. These values are a little higher with respect to our needs. Nevertheless, the present industrial production has been improved and the expected peak-to-valley error on one-meter scale is of the order of 50 microns. Additionally a selection procedure can be introduced.

As the thickness variation could introduce additional errors in the optical performances of the integrated glass in case an indirect integration process is used, the quality of the glasses has been measured. The thickness and the thickness variations have been measured thanks to the CHR600 sensor present on the CUP. As the thickness of the glass falls in the measurement range in thickness mode, it was possible to acquire an entire map in all the glasses area. The results are shown in figure 5. For each glass are shown the total thickness data and the thickness variation with respect to a flat, that corresponds to a tilt between the two surfaces. The thickness for all the glasses is around 198microns while the thickness variations are of the order of 2-3micron. Given the preferable direction recognizable in all the glasses, the impact of these features can be decreased with a good choice in the glass orientation.

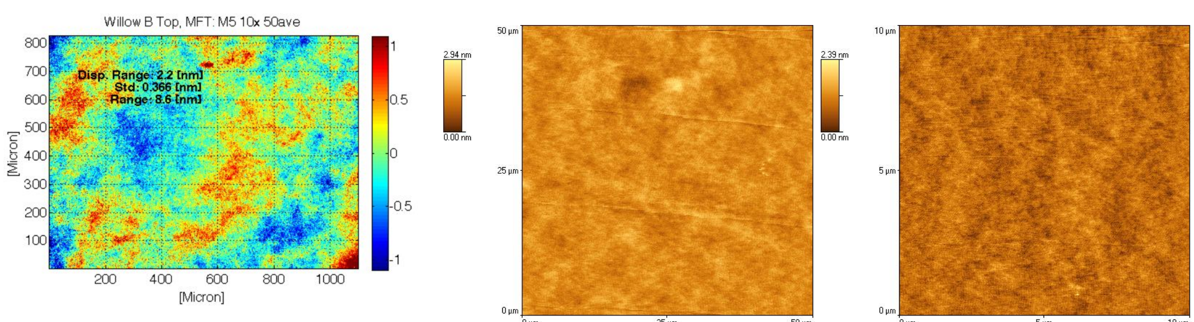

Figure 6: (A) An example of the images (color scale in nm) acquired on the Willow surface with the MFT (10x objective). The surface is 0.366 nm rms on the mm scale. (B) and (C): the surface as observed with the AFM on 50microns and 10microns scale, with rms(50μm)=0.23 nm, rms(10μm)=0.24 nm. The color scale is always in nm.

In the proposed process, avoiding the hot slumping process of the glasses, the segments can be coated and then directly integrated. The initial micro-roughness of the substrate is very important for the final micro-roughness after the coating.

The characterization of the micro-roughness has been carried out with 2 instruments: Micro-Finishing-Topographer (MFT), recently acquired by INAF/OAB and Atomic Force Microscope (AFM). An example of the acquired map for each magnification is shown in figure 6. The glass surface is extremely smooth: the resulted values, well below 0.5nm up to 1mm scale, make this kind of glass a suitable substrate for multilayer coating.
The very low initial micro-roughness of these glasses is more important for high energy application, at energies greater than 10keV: in this case the cold replication approach represents a key process and is very attractive for many high-throughput optics applications.

4 X-RAY MIRROR MODULE ASSEMBLY OPTICAL DESIGN

In order to show the potentiality of this assembly concept, an x-ray module has been designed accordingly to the proposed technology. As a benchmark, it has been used the Chinese X-ray Timing and Polarization mission (XTP) [13]. The mission includes a High energy X-ray Focusing Array (HFA), a Low energy X-ray Focusing Array (LFA), a High energy X-ray Collimated Array (HCA) and Wide Field Camera. The HFA with a focal length of 5.5 m is located in the middle of the satellite platform. The X-ray optics is a quasi-Wolter I type, focusing x-rays in the range of 1–30 keV with an angular resolution of about 1 arcminute and a field of view of 16 arcminutes. The effective area is 4000 cm2 @ 2-6 keV and 300cm2 @ 30 keV. The LFA telescope is composed by several mirror modules with a maximum aperture of 450 mm each with a focal length of 4.5m. The desired angular resolution of each module is not so tight, while the effective area and the weight are much demanding, being required 40kg maximum for each module. A summary of the requirements to be fulfilled for one of the LFA modules, used in the following, is reported in table 1.

Parameter	For one telescope
Focal length	4.5 m
Aperture	450 mm
Envelope	<=550 mm in diameter
Effective area on axis	>500 cm² @ 2-6 keV
Energy range	0.5~10 keV
Field of View	+/-8 arcmin (for 8 telescopes) +/-6 arcmin (for 2 telescopes)
Angular resolution (FWHM)	1 arcmin (for 8 telescopes) 15 arcsec (for 2 telescopes)
Mass(including structure)	<=40 kg
Working temperature	20+/-5 °C

Table 1: XTP LFA mission requirements table.

In table 2 the main mechanical parameters to build up the optical design are summarized. In the radial direction there is a stiffening partition, located at 97mm with respect to the optical axis. In correspondence of this partition, the number of sector in azimuthal direction changes from 3 to 6. In order to maintain the azimuthal correspondence between the ribs, a fixed number of ribs per sector is considered. Therefore the distance between the ribs is not constant and varies with the radius. At this preliminary stage of the design, no particular optimization has been considered for their positions and six ribs per section are considered. Two main stacks of glass compose radially the module, one between 26.3mm and 94mm (Inner part), the other between 100mm and 223mm (Outer part).
On the left side of figure 7 are reported the optical angular percentage available and the glass thickness as a function of the radius, it ranges from 70.8% to 91.8% with the outermost shell more effective. The glass thickness ranges between 30microns and 200microns: 30 microns thickness segments are necessary only for radius lower than 80mm. On the right side of figure 4 the reflectivity of different coating at different energies is reported as function of the incidence angle used for the effective area calculation. The optical design is segmented. There is a gap between the parabolic and hyperbolic sections of 20mm. The field of view is greater than 6'. The focal length is 4.5m and the length of the parabolic and hyperbolic section is 200mm. In figure 8 are shown the mirror profiles configuration, the effective area and the cumulative effective area for the inner and the outer parts of each module.

	Inner part	Outer part
Radial limit	26.3-94 mm	100-223 mm
Num sector in azimuthal direction	3	6
NumShell	68	57
% optics	78-84%	80.7-91.8%
Number of ribs per sector	6	6
Ribs distance	10-36mm	19.6-43.8mm
GlassWeight	≈ 1.2kg	≈7.5 Kg
GlassThickness	0.03-0.1mm	0.1-0.2mm
RangeRibThickness	≈ 0.65-1.45mm	≈ 1.6-3mm
WeightRib	≈ 1.2Kg	≈ 5Kg

Table 2: Inner and outer part main characteristics.

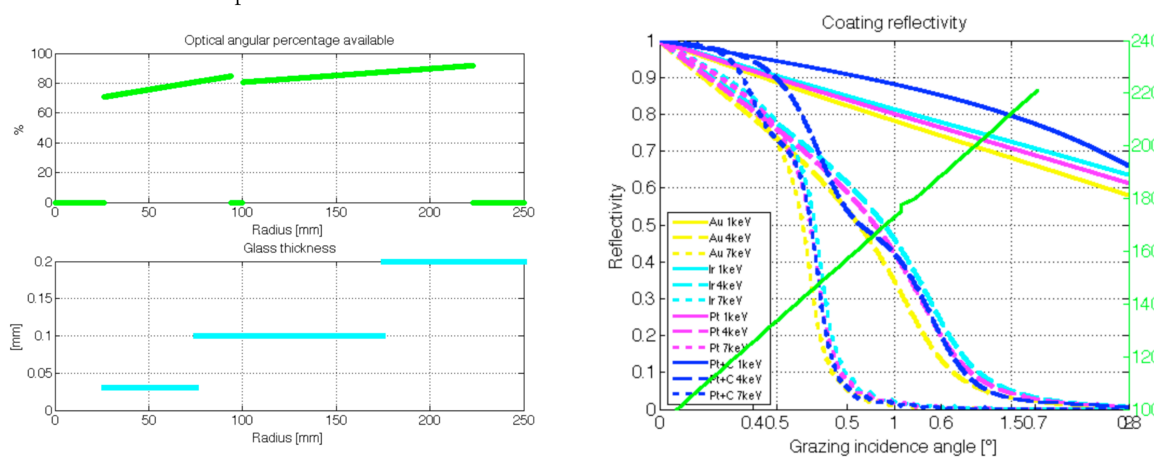

Figure 7: Left, Optical free angular percentage and glass thickness. The thickness is 30 microns, 100 microns and 200microns depending on the radius of curvature. Right, Coating Reflectivity versus incidence angle.

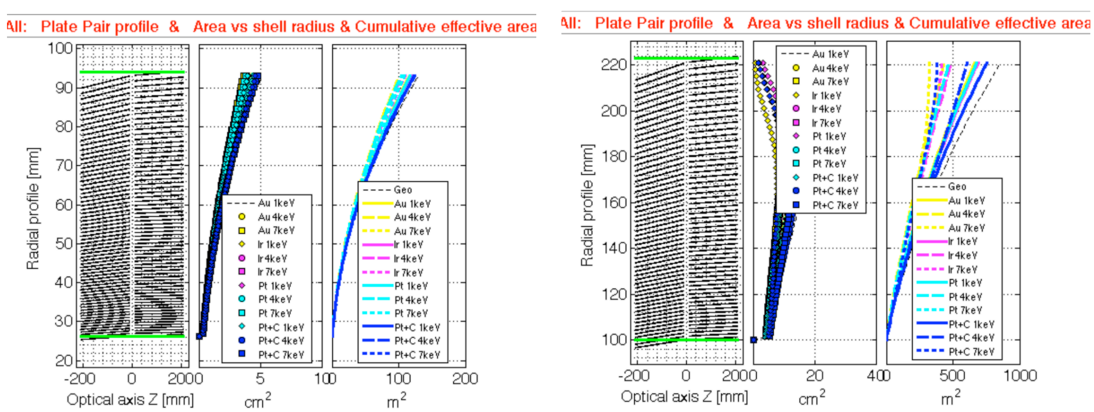

Figure 8: Mirror profiles, effective area per shell and cumulative area for inner and outer parts.

	Inner part	Outer part	All
Effective area @1keV (cm^2)	123.09	756.75	879.84
Effective area @4keV (cm^2)	124.09	605.05	729.14
Effective area @7keV (cm^2)	122.92	380.075	502.99

Table 3: Inner and outer part effective area

The effective area for the two radial partitions and for the overall assembly is reported in table 3: the values are given for the Pt+C case. The effective area is well above the requirements at low energies (e.g. greater than 500cm^2 between 1 and 6 keV): the number of the shells in the outer section can be decreased, reducing further the weight in a second phase, once the mechanical design of the system is confirmed. Nevertheless, the results in terms of mass for the whole module are quite promising. In table 4 are reported the materials and the weight of the different parts of the module. The total mass of the module is around 36kg, well in line with the required value (<40kg). This preliminary optical and mechanical design for the mirror module for the LFA of the XTP fulfills the given requirements in terms of mass and effective area.

Parts	Material	[kg]
Spiders	Titanium	5.57
Internal shaft	Invar	1.92
Ribs	Graphite	6.55
Shells	Willow	6.60
mid and back planes	Borofloat33	6.58
Blades	Invar	0.64
Case	Invar	7.98
TOT:		35.85

Table 4: LFA mirror module based on glass: materials and weight.

In order to allow the comparison between this cold slumping approach with the traditional electroforming nickel replica, a preliminary opto–mechanical design has been realized for this standard case. The simple optical module design is based on the Media Lario's manufacturing technology of Nickel electroforming, used for the optical modules of SAX, JET-X, XMM-Newton, and recently for eROSITA. From a general point of view, the angular resolution of 60 arcsec or better is definitely achievable with this well-proven technology. Nevertheless, as soon as the mirror thicknesses need to be reduced to limit the weight of the module, the mirror shell stiffness, which is mostly a function of the ratio between the mirror wall thickness and the shell radius, could be not sufficient to guarantee the result. In order to fulfill the requirement in terms of weight, the selected τ/R value has to be reduced to 0.8×10^-3 (3.5×10^-3 was the value adopted for XMM with an HEW = 15 arcsec, while 1.75x10^-3 was adopted for NHXM/SIMBOL-X). Minimum thickness is set to 100micron while maximum thickness is around 200micron. The angular resolution is also a function of the length of the shells, because the figure error usually concentrates at the mirror shell ends, therefore shorter mirror shells are typically more affected by deformations arising from the stress in bulk Nickel. Long shells also increase the effective area, thereby reducing the number of mandrels to be manufactured: a 300 mm length for both parabolic and hyperbolic segments has been selected. The adopted assumptions on the final structure are that the mirrors are attached to a 12-spokes spider obstructing 10% of the effective area made of Aluminium RSP and that the module is enclosed into a case made of Aluminium RSP.

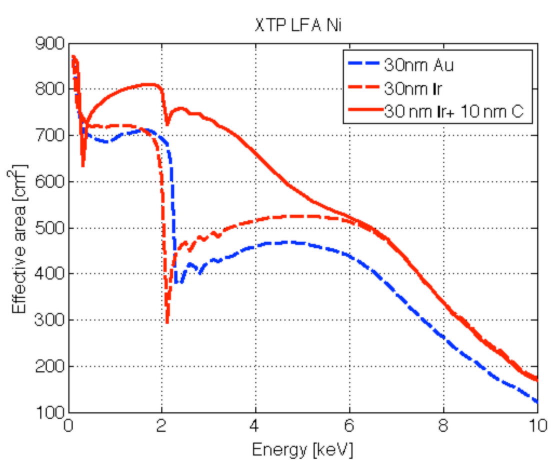

Figure 9: Effective area for a LFA module based electroformed nickel technology.

The effective area is evaluated with different coating: Gold 30 nm thick, Ir 30nm and Ir 30nm +C 10nm, assuming a 5 Å equivalent roughness (RMS). The results in terms of effective area are shown in figure 9, while the mass budget for a mirror module is summarized in table 5. In principle, the requirements in terms of effective area can be met, but in order to limit the mass budget, the required shell thickness is very demanding with no margin.
This comparison shows clearly the potentiality of the new proposed concept: the glass mirror module is 15% lighter than the nickel one, maintaining additional effective area of around 50cm^2 at all the energies.

Parts	**Material**	**[kg]**
Spiders	Alluminium RSP	3.5
Shells	Nickel	29
Case	Alluminium RSP	7.5
TOT:		40

Table 5: LFA mirror module based on electroformed nickel: materials and weight.

5 FIRST INTEGRATED MODULE RESULT

A first demonstrator for this new kind of mirror module has been realized using the present set-up used for the SGO as no modifications have been implemented so far in the IMA. A prototypal optic, called Willow Prototype 0 (WP0) has been realized by means of two of the glasses acquired. The integration followed in this case the standard approach with convex integration moulds, made in BK7 corresponding to a plate pair with radius of curvature of 1m at the intersection plane and a focal length of 20m. As a first trial, in order to limit the number of new items to be acquired, already available ribs in BK7 have been used. The same approach has been used for the spacing, operated using the same alignment mask and therefore following SGO prescription. Moreover, an aluminum backplane has been used. This configuration is clearly not optimized with respect to the optical performances of the integrated glass. Nevertheless it has been useful to have a first feedback on the glass handling procedure as well as on the achieved results in comparison to simulations.
A picture of the WP0 and the residual profile acquired with the CUP profilometer are shown in figure 10. For both the parabolic and the hyperbolic segment the inferred HEW is given. The central part of each of the two segments is around 20-30 arcsec in single reflection. The results are quite promising. Further analyses are under development to enable a reliable simulation algorithm, necessary for the optimization of the opto-mechanical design. These values are even better than what was originally expected from FEM simulations.
In the future, the repeatability of the results, the stacking procedure with several glasses, the multi-layer deposition process and the coated layer integration process will be investigated. As well, integration molds with different focal lengths and smaller radius of curvature explored.

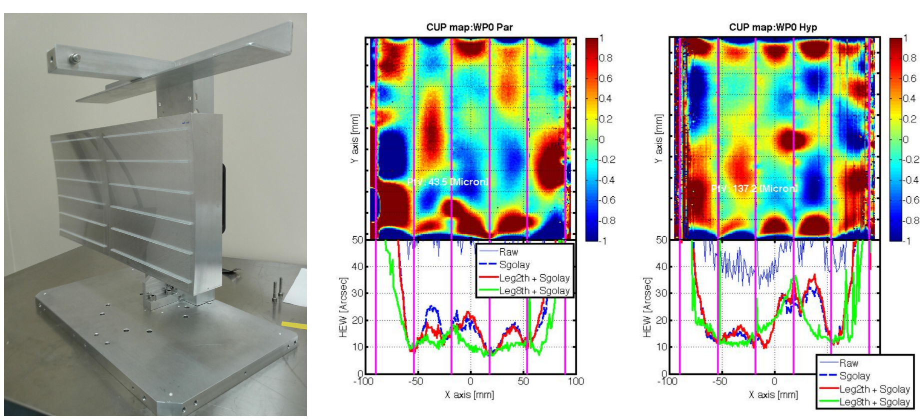

Figure 10: First integrated prototype based on thin glass cold slumping technology.

6 CONCLUSIONS

The traditional SGO approach is based on a two steps process. In the first part the glass are slumped (to Wolter-I or cylindrical configuration), while they are assembled into a structure in a second phase. The new concept, described in this paper, proposes to skip the hot slumping procedure and go straight to the integration procedure. The mass production of very thin glass foils (0.03-0.2mm thick) is now pursued by several industries. The Willow glass (thickness of 0.1-0.2 mm) produced by Corning and the AF32 produced by Schott (thickness of 0.055 mm) are good examples. Thanks to their thickness, strength and flexibility they can be bent to very small radius of curvature without breaks. This feature, together with the very low micro-roughness, makes this kind of materials ideal candidates for pursuing a cold replication approach for cost-effective and fast making of grazing incidence astronomical optics.

Starting from the very thin flat glass sheets, the assembly concept, based on the use of Wolter-I counter-form moulds and on the use of reinforcing ribs, it is possible constrain the foil profile to the correct shape during the bonding.

The reduced cost production and the low weight of these glass mirror modules make this technology very attractive for the production of high throughput optics. The process has been patented. The gain that this new approach allows has been shown comparing, as an example, a preliminary opto-mechanical design for the LFA of the Chinese XTP mission based on electroformed nickel technology and on the CSGO approach. In order to fulfill the requirements in terms of weight, the thickness of the shell in nickel have to be reduced a factor four with respect to XMM. It can be probably done at the expenses of the angular resolution performances; nevertheless there is no margin in the total weight of the mirror module. On the other side, the CGSO concept, even allocating a complete and reliable mass budged for the whole structure, allows to keep some margin with respect to the 40kg limit. It is around 15% lighter than the nickel one. Moreover, a Half Energy Width in the range of 20-60 arcsec is compatible with the expected residual error due to the spring back of the glass sheets. The results achieved with the first demonstrator realized with this new approaches are quite promising. Further investigations with respect to FEM simulations and prototype realizations will be carried out in the next months to fully explore the potentiality of the process.

ACKNOWLEDGMENTS

Many thanks to all OAB staff (in particular to S. Cantù and E. Mattaini of the OAB mechanical workshop) for their valuable support.

REFERENCES

(1) F.A. Harrison, et al., "The Nuclear Spectroscopic Telescope Array (NuSTAR)", Proc. SPIE 7732, (2010) 10.1117/12.858065

(2) W. Zhang, et al., "Lightweight X-ray Mirrors for the Constellation-X Mission," Proc. SPIE 6266, (2006)

(3) M. Ghigo, S. Basso, R. Canestrari, P. Conconi, O. Citterio, M. M. Civitani, E. Dell'Orto, D. Gallieni, G. Pareschi, G. Parodi, L. Proserpio, D. Spiga, "Hot slumping glass technology and integration process to manufacture a grazing incidence scaled prototype for the IXO telescope modules", Proc. SPIE 7437, (2009)

(4) Kai-Wing Chan, et al, "An approach for alignment, mounting, and integration of IXO mirror segments," Proc. SPIE 7437, 74371D (2009)

(5) M. M. Civitani, S. Basso, M. Bavdaz, O. Citterio, P. Conconi, D. Gallieni, M. Ghigo, B. Guldimann, F. Martelli, G. Pagano, G. Pareschi, G. Parodi, L. Proserpio, B. Salmaso, D. Spiga, G. Tagliaferri, M. Tintori, E. Wille, A. Zambra, "IXO x-ray mirrors based on slumped glass segments with reinforcing ribs: optical and mechanical design, image error budget, and optics unit integration process", Proc. SPIE 7732, (2010)

(6) M. M. Civitani, S. Basso, O. Citterio, P. Conconi, D. Gallieni, M. Ghigo, G. Pareschi, L. Proserpio, B. Salmaso, G. Sironi, D. Spiga, G. Tagliaferri, A. Zambra, F. Martelli, G. Parodi, P. Fumi, M. Tintori, D. Gallieni, M. Bavdaz, E. Wille, "Accurate integration of segmented x-ray optics using interfacing ribs", Opt. Eng. 52(9), 091809-091809, (2013)

(7) K. Nandra, X. Barcons, D. Barret, A. Fabian, J.W. den Herder, L. Piro, M. Watson "Athena: The Advanced Telescope for High Energy Astrophysics", Mission proposal, http://www.the-athena-x-ray-observatory.eu/

(8) G. Parodi, F. Martelli, S. Basso, M. Bavdaz, O. Citterio, M. M. Civitani, P. Conconi, M. Ghigo, G. Pareschi, L. Proserpio, D. Spiga, E. Wille, A. Zambra, "Design of the IXO optics based on thin glass plates connected by reinforcing ribs", Proc. SPIE 8147, (2011)

(9) M. M. Civitani, S. Basso, M. Ghigo, D. Spiga, B. Salmaso, G. Pareschi, G.Vecchi, V. Burwitz, G. D. Hartner, B. Menz, "Slumped Glass Optics based on thin hot formed glass segments and interfacing ribs for high angular resolution X-ray astronomy: performances and development status," Proc. of SPIE Vol. 9603, (2015)

(10) M. M. Civitani, S. Basso, M. Bavdaz, O. Citterio, P. Conconi, D. Gallieni, Ghigo, M., B. Guldimann, F. Martelli, G. Pagano, G. Pareschi, G. Parodi, L. Proserpio, B. Salmaso, D. Spiga, G. Tagliaferri, M. Tintori, E. Wille, A. Zambra, "An integration machine for the assembly of the x-ray optic units based on thin slumped glass foils for the IXO mission", Proc. SPIE 8147, 81470R (2011)

(11) M. Civitani, M. Ghigo, S. Basso, L. Proserpio, D. Spiga, B. Salmaso, G. Pareschi, G. Tagliaferri, V. Burwitz, G. D. Hartner, B. Menz, M. Bavdaz, E. Wille, "Direct hot slumping and accurate integration process to manufacture prototypal X-ray Optical Units made of glass", Proc. of SPIE Vol. 8861 886110-1 (2013)
(12) M. M. Civitani, M. Ghigo, O. Citterio, P. Conconi, D. Spiga, G. Pareschi, L. Proserpio, “3D characterization of thin glass x-ray mirrors via optical profilometry”, Proc. SPIE 7803, 78030L (2010)
(13) Zhanshan Wang et al. , “Development of the X-ray Timing and Polarization telescope optics”, Proc SPIE 9144, 91441E (2014)